



OPEN

Characterizing the effects of structural fires on fine particulate matter with a dense sensing network

Ayina Anyachebelu¹✉, Alex Cabral², Marah I. Abdin³, Pallavi Choudhury³ & Madeleine I. G. Daep³

Short-term increases in air pollution levels are linked to large adverse effects on health and productivity. However, existing regulatory monitoring systems lack the spatial or temporal resolution needed to capture localized events. This study uses a dense network of over 100 sensors, deployed across the city of Chicago, Illinois, to capture the spread of smoke from short-term structural fire events. Examining all large structural fires that occurred in the city over a year ($N = 21$), we characterize differences in $PM_{2.5}$ concentrations downwind versus upwind of the fires. On average, we observed increases of up to $10.7 \mu\text{g}/\text{m}^3$ (95% CI 5.7–15.7) for sensors within 2 km and up to $7.7 \mu\text{g}/\text{m}^3$ (95% CI 3.4–12.0) for sensors 2–5 km downwind of fires. Statistically significant elevated concentrations were evident as far as 5 km downwind of the location of the fire and persisted over approximately 2 h on average. This work shows how low-cost sensors can provide insight on local and short-term pollution events, enabling regulators to provide timely warnings to vulnerable populations.

Air pollution is the leading environmental risk factor for morbidity and mortality globally¹. All but 1% of the world's population breathes air exceeding World Health Organization air quality limits², with inequitable exposures implicated in disparities in respiratory and cardiovascular disease^{3,4}, adverse pregnancy outcomes^{5,6}, and other morbidities^{7,8}. Less is known, however, about the contributions of short-term and localized events to air pollution burdens.

Short-term ambient air pollution events adversely impact health^{9–11} as well as productivity¹². Even small increases in fine particulate matter ($PM_{2.5}$) concentrations over periods as short as 2 hours are associated with increased heart attack and stroke risk¹³. Short-term and localized exposures may also be more easily mitigated than chronic exposures, for example via timely warning systems that lead people to close windows to prevent indoor infiltration¹⁴ and to postpone outdoor activities¹⁵. However, transient and local events are often undetected by regulatory monitors, which are sparsely distributed across cities¹⁶. Many regulatory monitoring systems also collect data infrequently or at coarse temporal resolutions, missing episodic emissions¹⁷, and extensive quality assurance processes can introduce delays between when an event occurs and when the public learns of its effects. A recent proliferation of low-cost air quality sensing networks promises to address these challenges, but existing research has tended to focus on monitoring sources known a priori in order to support local advocacy agendas^{18,19} or on generalized anomaly detection^{20–22}, rather than on capturing unpredictable events. This paper seeks to fill this research gap by showing how a large-scale, low-cost sensor network can characterize the changes in $PM_{2.5}$ concentrations associated with structural fires in a major city over a full year of observation.

Structural fires—fires involving the structural component of various types of residential, commercial, or industrial buildings—are an important yet under-monitored cause of short-term and localized pollution episodes. In the United States, there are approximately half a million structural fires every year²³. But structural fires are unpredictable events that rarely occur immediately upwind of a regulatory monitor, and thus the few studies seeking to better quantify their impacts have focused on major industrial accidents^{24–26}. To our knowledge, there is no research on increases in $PM_{2.5}$ concentrations associated with general structural fires that, although smaller, are far more frequent²³. Moreover, although an extensive literature has documented socioeconomic and racial inequities in the locations of fires as well as in their contributions to property damages, injury, and mortality^{27,28},

¹Department of Civil, Environmental and Geomatic Engineering, University College London, London WC1E 7HB, UK. ²John A. Paulson School of Engineering and Applied Sciences, Harvard University, Boston, MA 02134, USA. ³Microsoft Research, Redmond, WA 98052, USA. ✉email: ucesaua@ucl.ac.uk

little research has examined inequities in their effects on pollution—which may considerably magnify health consequences, particularly if the nearby population is affected by pre-existing health vulnerabilities.

In this paper, we show how a network of low-cost sensors can fill key monitoring gaps. We characterize effects on PM_{2.5}, which is one of many pollutants that fires emit, for three reasons: (1) PM_{2.5} has been shown to affect health even at low levels^{7,29}; (2) the PM_{2.5} from fires may be particularly health-hazardous because it contains trace metals and other harmful byproducts of the burning of synthetic materials^{30,31}; and (3) innovations in optical particle sensing and sensor calibration increasingly enable reliable low-cost measurement of PM_{2.5} concentrations³², making it possible for us to deploy a network with frequent readings and spatially dense monitoring³³. We combine in-situ PM_{2.5} observations with meteorological observations of wind direction to compare concentrations downwind versus upwind of structural fires, applying a difference-in-differences approach to characterize the average time period over which smoke persists. Our findings demonstrate the promise of low-cost sensor networks to characterize health-relevant, hyperlocal changes in PM_{2.5} that routine environmental monitoring systems have previously struggled to detect.

Data

To obtain air quality data, we deployed a network of 115 low-cost wireless sensing nodes across Chicago bus shelters. Named Project Eclipse, the initiative was a collaboration with partners including the Chicago Department of Public Health and JCDecaux Chicago, the local affiliate of the global advertising agency JCDecaux SA, the world's largest provider of outdoor street furniture. The original goal of the network was twofold: first, to provide citywide coverage that could support the data needs of city and academic researchers; and second, to provide additional monitoring in environmental justice neighborhoods where residents have historically been underserved by environmental monitoring³³. The resulting network was more spatially dense than existing routine environmental monitoring systems: the average Chicago resident lived within 0.65 miles of one of our sensing nodes compared to 1.6 miles and 3.3 miles from crowd-sourced and regulatory monitors, respectively³³.

Briefly, Eclipse devices report measurements of PM_{2.5}, collected every 5 min using a Sensirion SPS30 optical particle sensor, as well as temperature, relative humidity, pressure, and a set of four gaseous pollutants. We deployed devices starting in July 2021. We determined locations using a three-step framework: first, we selected 80 sites identified using a stratified random sampling design following Matte et al.³⁴; second, we worked with community groups and local partners to select 26 additional sites in environmental justice areas; and finally, we co-located 3 additional devices with each of three regulatory monitoring stations (n = 9 devices total). Because low-cost optical particle sensors can be subject to error, the research team used these co-located devices to develop a calibration algorithm that improved accuracy to levels consistent with EPA recommendations for low-cost sensors³⁵. We have included a detailed description of the calibration method and results in Appendix A of the supplementary information. For further details on the network design and hardware, please see Daepf et al.³⁶; the calibrated data and further details on the calibration method are publicly available³⁷.

To identify structural fires, we collected all fire reports posted to the City of Chicago Fire Department's public Twitter page between July 1, 2021 and June 30, 2022³⁸. Posts include each fire's location (street address), start time, and alarm level—a rating from 1 to 3 indicating the amount of units and firefighters needed to contain the fire, where 3-alarm fires were the largest observed in Chicago during the study period. Although the listing of 1-alarm fires was not comprehensive, the Fire Department Media team confirmed that the list included all 2- and 3-alarm fires in the study period; for the purpose of this paper, we thus constrain our analyses to the multi-alarm fires. To ensure the accuracy of each variable, we further cross-referenced the data against local news reports for each fire. We then geocoded locations using Nominatim (OpenStreetMap)³⁹.

Finally, we obtained meteorology data from the National Oceanic and Atmospheric Administration (NOAA) via the Meteostat weather database⁴⁰, which included data from two NOAA weather stations in Chicago (Figure 1 Panel A). We linked each sensor reading with the wind direction, wind speed, temperature, and precipitation of the weather station closest to the corresponding fire.

Our raw structural fire data set includes 23 multi-alarm fires from July 2021 to July 2022. We further remove 2 fires that occurred at a time with no dominant wind direction. For the remaining 21 multi-alarm fires, we obtain 152,275 PM_{2.5} readings from all sensors during the 3 h before and after the fires. Following Lu et al.⁴¹, we apply a three-step quality assurance/control procedure. First, we exclude PM_{2.5} outliers with abnormal 5-min values equal to or less than 0 μg/m³ or greater than 1000 μg/m³ (0.01%) to mitigate the effects of sensor malfunctions. Second, to further ensure the exclusion of malfunctioning devices, we remove sensors with less than 75% of the 73 readings expected during the 6-hour monitoring period of each fire (1.19%). Finally, to account for skipped readings, we impute missing readings within a given sensor using linear interpolation. Our final data set has 156,667 5-min readings for the 3 h before and after the 21 fires.

Methods

We use a difference-in-differences estimation approach to evaluate the effects of structural fires on PM_{2.5} readings, comparing concentrations observed using sensors downwind versus upwind of each fire after versus before the fire's start. This approach exploits the role of wind direction, which dictates the local transport of pollutants^{9,42,43}, to control for potential sources of confounding variables. Fires may, for example, be more likely to occur in neighborhoods that also have higher baseline levels of PM_{2.5}; however, both the downwind and upwind sensors would be similarly affected, and thus the upwind sensors would act as a control for the relatively higher readings that would have been expected even in the absence of a fire. Similarly, a citywide pollution event could coincide with the start of a fire—but the increase in concentration would be observed in the upwind as well as the downwind sensors, and thus would not affect the estimated difference. The identifying assumption is thus that any factors besides the fires that contribute to short-term changes in PM_{2.5} (including other local pollution sources

or gradients of other pollutants that influence secondary organic aerosol production) are not consistently either upwind or downwind of fires but rather distributed at random, and thus do not bias the difference-in-differences estimator across the population of fires.

Identifying downwind and upwind sensors. Given the limited literature on fire plumes in urban areas, we choose to create a simplistic version of a plume that can generalize to the 21 structural fires included in the analyses. Using the average building height and road width in Chicago^{44,45}, we determine that the average street has a medium ratio of road width to building height, thus resulting in moderate flushing rates of $PM_{2.5}$ based on the air flow and potential to concentrate locally-emitted pollution⁴⁶. As a result, we use a wide rectangular band in the direction of the fire (Fig. 1 Panel B) to represent the fire plume—wide to acknowledge the dispersion on roads that are not street canyons, and rectangular to accommodate the air flow patterns. We set the width of the band to 1 km in the primary analysis, a distance that enables the inclusion of more downwind sensors in comparison to smaller widths but excludes unaffected sensors indicated by the similar but diminishing effect sizes with wider bands in robustness tests (see Results for further details).

To determine the control group—hereafter referred to as upwind sensors—we consider any sensors at least a 90 degree angle away from the wind direction as upwind. That is, sensors are classified as “upwind” of a given fire if they are located within the semi-circle in the opposite direction of the prevailing wind, as shown in Fig. 1. We consider any sensors in the downwind band as downwind. As a result, a sensor can be considered as a downwind sensor for one fire and upwind sensor for a different fire. We examine the association of measurements with distance from the fire by calculating bands of lengths 2, 5 and 10 km. To ensure that the upwind sensors reflect a comparable control group (e.g. for neighborhood-specific concentrations levels) to the downwind sensors, we restrict our analysis to sensors that are within 5 or 10 km of fires.

For all 21 multi-alarm fires that are used in the analyses, 16 (76%) have at least one downwind sensor within 10 km and 14 (67%) have a downwind sensor within 5 km. On average, each fire has 2.1 and 2.5 downwind sensors within 5 km and 10 km respectively.

Before conducting our main analyses, we compared the trends in $PM_{2.5}$ readings *before* the start of the fires. The difference-in-difference approach relies on the identifying assumption that the treatment and control groups (downwind and upwind sensors) would have followed parallel trends in the absence of a fire. Figure 2 plots the trends for the average 5-min readings of $PM_{2.5}$ for the sensor groups during the 3 h before and after the fires

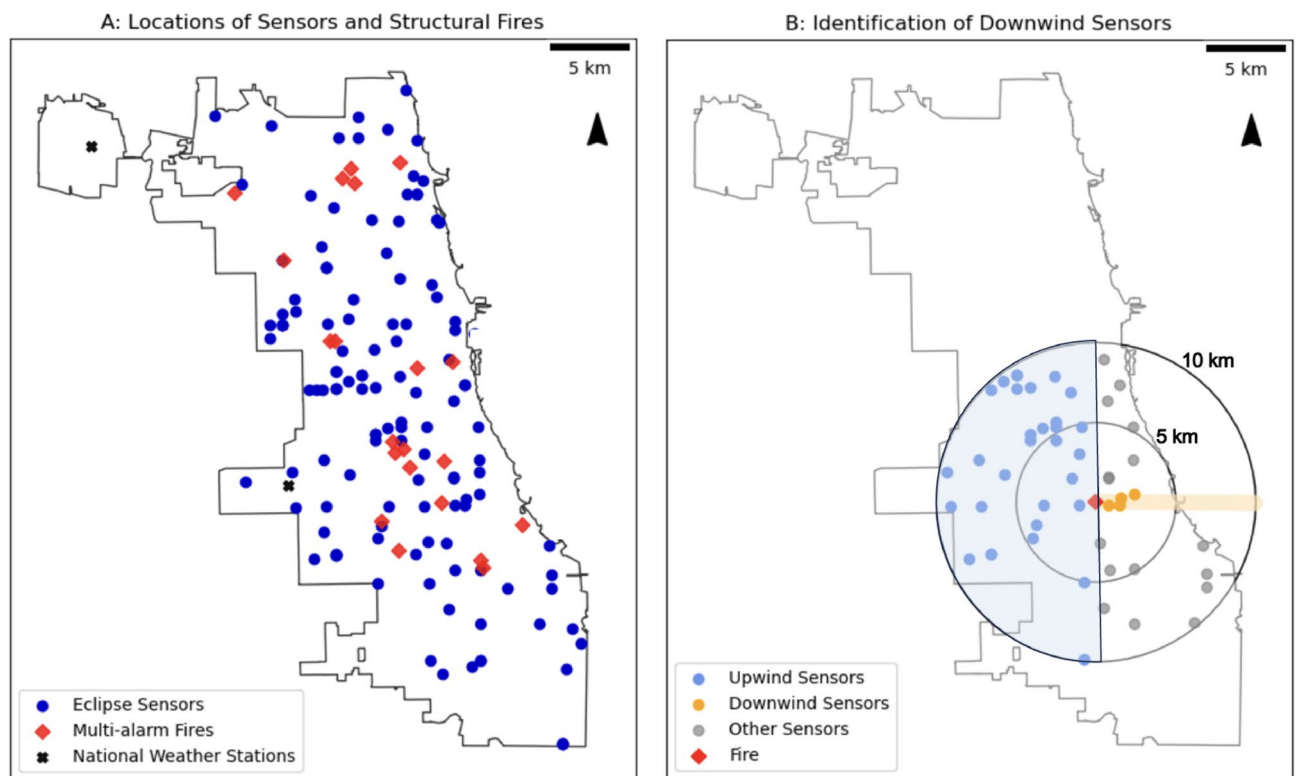


Figure 1. Panel (A): Locations of Eclipse sensors (blue points), multi-alarm fires (red diamonds), and NOAA Weather Stations (black crosses) within the entire city limits of Chicago. Panel (B): Identification of Downwind and Upwind Sensors For One Fire. Black circles are radii of 5 km and 10 km from the fire. Sensors falling within these circles are used in the analysis. The rectangular orange band represents the fire emissions path in direction of the wind (east). Sensors that fall into the band (orange points) are labelled as downwind, sensors that fall into the highlighted semicircle (blue points) are upwind, and all other sensors (grey points) are not included in the analysis.

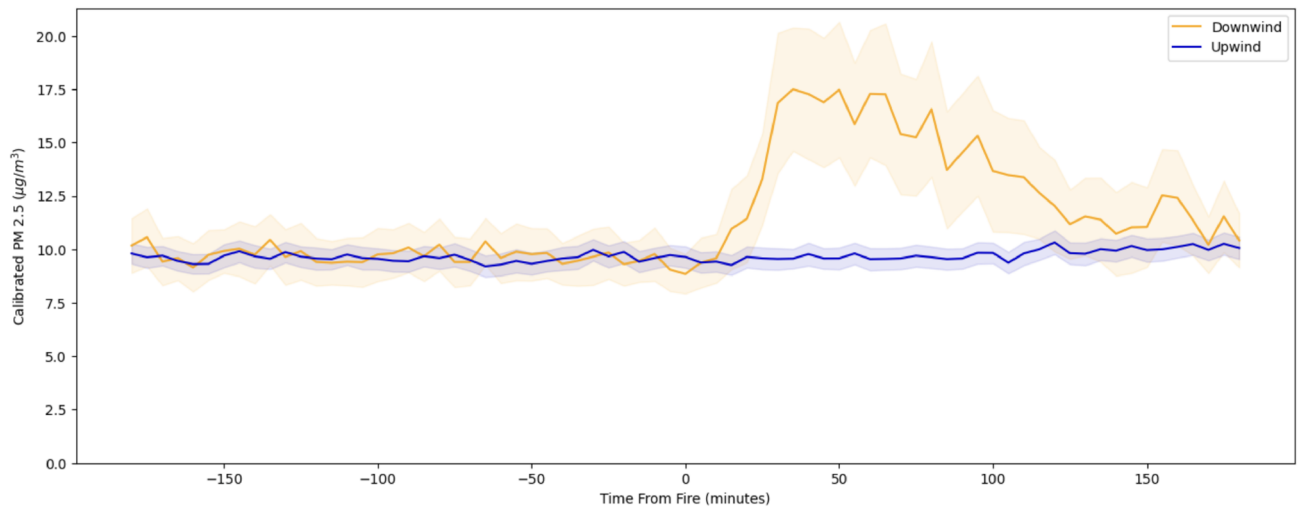


Figure 2. Parallel Trends Plot: Average calibrated $PM_{2.5}$ readings for downwind and upwind sensors before and after fires. Lower and upper bounds of confidence intervals are 2 standard errors from the mean. All sensors included in the figure are within 5 km of fires. Number of downwind sensors = 29. Number of upwind sensors = 312.

(Fig. 2). Although we cannot test the assumption, evidence of parallel trends in the pre-period—before the fire—bolsters confidence that the assumption holds.

Model. We estimate the relationship between structural fires and calibrated $PM_{2.5}$ for sensor i at time t using the model:

$$PM_{it} = \alpha + \sum_{k=-35}^{-1} \beta_k \text{Downwind}_{it}^k + \sum_{k=1}^{35} \beta_k \text{Downwind}_{it}^k + X'_{it} \Gamma + \mu_i + \lambda_t + \varepsilon_{it} \quad (1)$$

We include a set of time-variant dummy variables, Downwind_{it}^k , to allow for a non-parametric period-specific effect of the fire. k ranges from -35 to 35 which indexes the 35 5-mi readings for the 180 min (3 h) before and after the fires. For each sensor, we have an equal number of readings before and after the fire, ensuring balanced data in our pre- and post- fire periods. The coefficients of interest, β_k , denote the difference in $PM_{2.5}$ between downwind and upwind sensors in the $5k_{th}$ minute. This approach enables us to examine how the effect changes over time. In addition to offering insight on the peak and duration of effects, we note that the lack of any observable trend in the resulting coefficients prior to the fire would offer further evidence of parallel trends in the pre-period.

To investigate how the effect on $PM_{2.5}$ varies over space, we also stratify the treatment group based on distance (0–2 km, 2–5 km, and 5–10 km) from the fire. We choose these distance bins to ensure that there are enough downwind sensors in each distance group for analysis. To control for sensor-specific factors, diurnal or seasonal variation, and fire-specific differences, our specification includes μ_i , a sensor-specific fixed effect, as well as λ_t , denoting time (month, hour and fire) fixed effects. Additionally, we run the regression including a vector of meteorological parameters, X'_{it} , including wind speed, temperature and total precipitation in the 24 h before the fire, given that several studies show that these meteorological factors influence $PM_{2.5}$ concentrations^{43,47–49}.

Finally, to examine inequities in the $PM_{2.5}$ burdens associated with fires, we estimate the average demographic makeup of areas affected by fire plumes relative to the demographic makeup of the city as a whole. For each fire, we identify all census block groups that overlap with the 5 km downwind bands; we then evaluate differences in the demographic characteristics (obtained from the 2016–2020 5-year American Community Survey) for affected versus unaffected areas⁵⁰.

We conduct several sensitivity analyses to probe the robustness of our results. Across models, we cluster standard errors at the sensor level; as an additional robustness check, we also fit models with clustering at the fire level to account for possible serial correlation within a fire. Because our data are derived from low-cost sensors—meaning that the estimated effect magnitudes may be subject to measurement error—we also fit the specification using the natural log of the outcome variable to observe relative effects. Finally, we rerun the analysis using a greater selection of upwind sensors that includes all sensors within 5 km that do not fall into the rectangular downwind band, to evaluate the robustness of our analysis to the way in which we identify upwind sensors. We further check the sensitivity of our results to our definition of downwind sensors by fitting models with several different widths for the rectangular downwind band.

Results

Figure 3 shows the estimated effect of multi-alarm structural fires on $PM_{2.5}$ over time. Comparing sensors that are downwind versus upwind and restricting our analysis to sensors within 5 km of the fire's location, we observe statistically significant differences after but not before the fire's start.

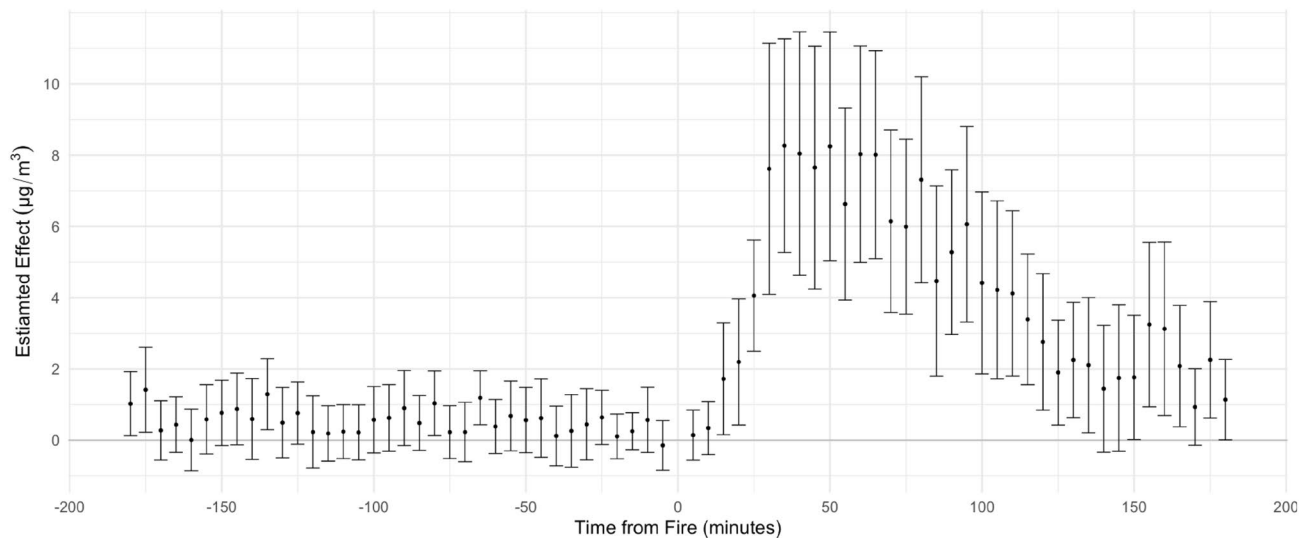


Figure 3. Model-estimated effect of structural fires on $\text{PM}_{2.5}$ Levels Using 1000 m wide and 5 km long downwind band. All sensors are within 5 km of the fire. Standard errors are clustered at the sensor level. Estimates are from model including time, fire-specific, and sensor-specific fixed effects and meteorological parameters. Number of Fires = 21. Number of downwind sensors = 29. Number of upwind sensors = 158.

Overall, sensors had an average reading of $10.2 \mu\text{g}/\text{m}^3$ (SD = 3.8) for the hour before the start of fires. The estimated difference in $\text{PM}_{2.5}$ readings of downwind versus upwind sensors increases after a fire's start. On average, $\text{PM}_{2.5}$ levels for downwind sensors begin increasing 15 min after the start of the fire and remain elevated for over 2 hours. The average peak, or largest difference, is a $8.3 \mu\text{g}/\text{m}^3$ 95% CI [5.2–11.2] increase in $\text{PM}_{2.5}$ that is observed approximately 35 min after the fire's reported start time. In general, $\text{PM}_{2.5}$ readings are approximately over $5 \mu\text{g}/\text{m}^3$ higher than the baseline from 30 to 100 min after the fire.

Effects are robust to a larger selection of upwind sensors and to the use of a range of different widths for the rectangular band identifying downwind sensors, as well as to the inclusion of fire fixed effects, and to two-way clustering of standard errors by fire and sensor (See Supplementary Information). We report results for the robustness checks in the Supplementary Information. We further note that the pre-fire coefficients from Fig. 3 are stable over time and not significantly different from 0, again bolstering our confidence with respect to the parallel trends assumption.

We next investigate the average spatial extent of the changes in $\text{PM}_{2.5}$. We stratify sensors by distance from each fire (Fig. 5). As expected, the observed increase in concentrations is smaller for sensors further from a given fire. Statistically significant increased readings are observed at downwind sensors 0–2 km and 2–5 km from fires, but not for sensors more than 5 km away. Sensors within 2 km had increases as high as $10.7 \mu\text{g}/\text{m}^3$ 95% CI [5.7–15.7]. Effects 2–5 km away are similarly persistent, albeit with smaller peaks corresponding to $7.7 \mu\text{g}/\text{m}^3$ 95% CI [3.4–12.0] increases in concentrations.

While the model estimates the effect on concentrations across all fires, the impact of individual fires varied. We observed differences in $\text{PM}_{2.5}$ as high as over $20 \mu\text{g}/\text{m}^3$ between the raw readings of downwind and upwind sensors after a singular fire. The average readings of downwind sensors for the individual fires can be found in the Supplementary Information.

Table 1 evaluates socioeconomic and demographic disparities in census block groups overlapping versus not overlapping the downwind bands. Affected census block groups have statistically significantly lower median incomes and relatively smaller White populations, on average. They also have higher proportions of Black residents and children under 6 years old. There are no significant differences in the proportion of Hispanic residents and elderly residents. Although factors such as local meteorology could affect these results, Fig. 4 shows that the locations of the fires coincide with the neighborhoods of the city with lower incomes and proportionally more Black residents—suggesting that these neighborhoods are more likely to experience fire-associated increases in $\text{PM}_{2.5}$ concentrations regardless of the direction of the wind at the time of the fire.

Short-term events may be of particular concern when they affect vulnerable groups. For this reason, we overlay the fire downwind bands with locations of schools and senior centers in Chicago^{51,52}. We find that the 5 km area downwind of fires included at least one school for every large fire, affecting approximately 1 in 5 of all Chicago public schools over the one-year period of observation. Similarly, 5 of the city's 21 senior centers were in the path of the downwind bands at least once.

Discussion

This study examines the effect of short-term structural fires on $\text{PM}_{2.5}$ concentrations. Using a spatially and temporally dense network of real-time $\text{PM}_{2.5}$ sensors, we are able to describe the spread and duration of heightened concentrations. We find that, on average, multi-alarm fires contribute up to a $10.7 \mu\text{g}/\text{m}^3$ increase in $\text{PM}_{2.5}$ within 2 km of a fire and a $7.7 \mu\text{g}/\text{m}^3$ increase 2 to 5 km away from a fire. The heightened concentrations lasted

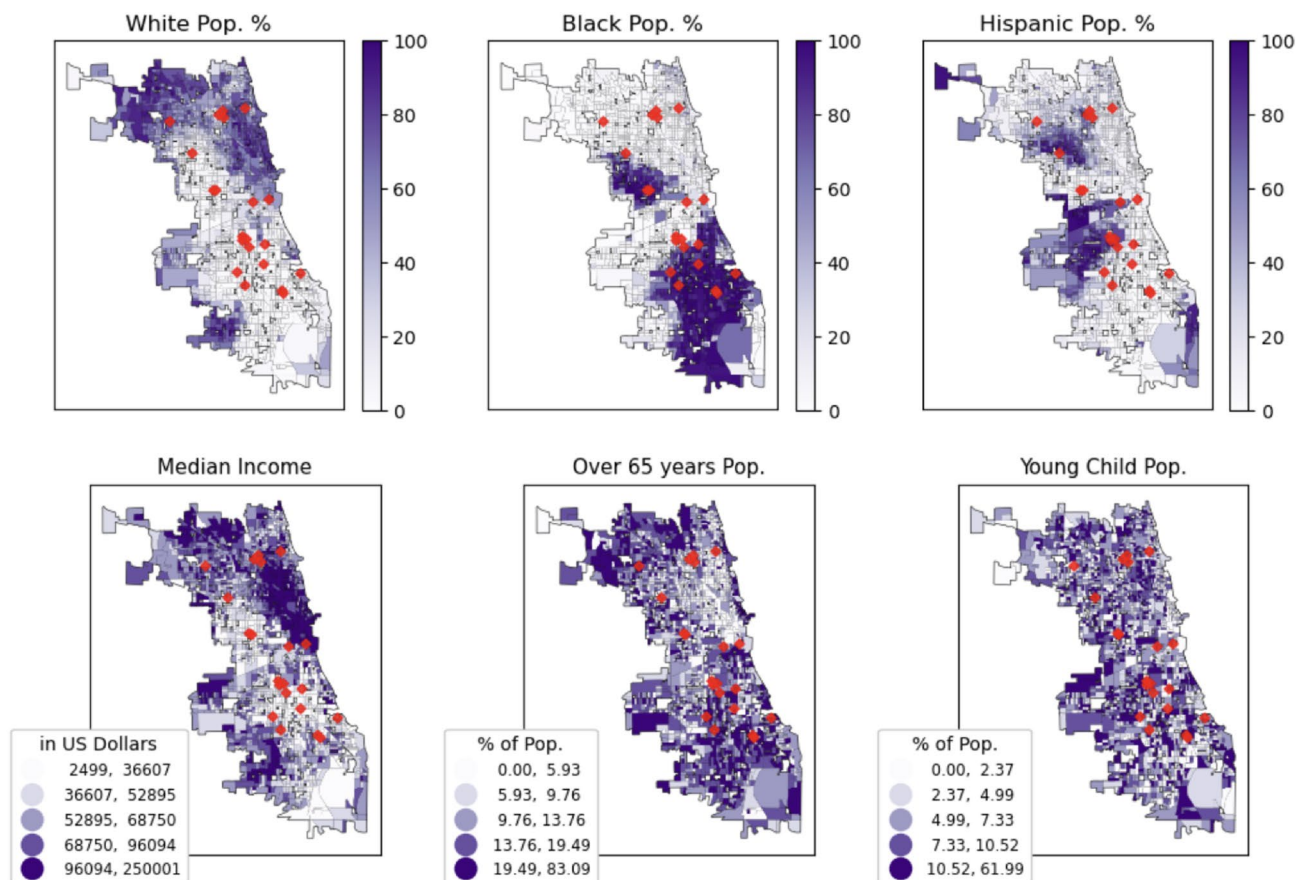


Figure 4. Locations of multi-alarm structural fires (red diamonds) and socioeconomic or demographic makeup in Chicago.

for approximately 2 h after the fire's start and disproportionately affect neighborhoods with lower incomes, relatively smaller White populations and larger Black populations, and relatively more children under 6 years old.

The observed increases in $PM_{2.5}$ associated with structural fires should be of concern to public health researchers and practitioners for three reasons. First, we observe statistically significant and large increases in $PM_{2.5}$ readings as far as 5 km from the location of fires. The changes in concentrations from a single fire could be much larger, surpassing $20 \mu\text{g}/\text{m}^3$ in some individual instances, and is likely much larger close to the fire's source. Considering research that even an additional $1 \mu\text{g}/\text{m}^3$ of exposure for a day leads to more hospitalizations, our results suggest that structural fires could be meaningfully contributing to adverse health outcomes⁹. Second, the observed increase in $PM_{2.5}$ persists for approximately 2 h on average—a duration that, although short, has been shown to result in negative health effects for vulnerable populations^{13,53}. Moreover, multi-alarm fires can last for several hours, suggesting that the impact on $PM_{2.5}$ likely extends beyond the time periods observed in this study.

Finally, we show that the downwind bands overlapped with areas of relatively larger populations of low-income and Black residents and young children relative to other parts of the city during the year-long period of observation, highlighting an additional burden that should be considered in addition to the existing literature on structural fires' inequitable effects^{27,28}. These increased concentrations may not directly translate into increased emissions burdens, because factors like residential mobility and air quality intrusion will mediate the extent to which increased outdoor concentrations in a particular neighborhood translate into increased exposures amongst its residents. However, prior research suggests that residents of low-income and racially segregated urban neighborhoods spend more time in their home microenvironments relative to residents of other neighborhoods^{54,55} and tend to live in older and less expensive houses that are subject to relatively higher rates of pollution infiltration⁵⁶, likely magnifying disparities in potential health impacts between disadvantaged and advantaged neighborhoods. Furthermore, our work finds that every downwind band affected at least one school—underscoring the potential of real-time monitoring and warning systems to mitigate students' exposures.

This study is subject to three key limitations. First, our study relies on low-cost sensors, which are subject to error⁵⁷. We thus limit our analysis to $PM_{2.5}$, for which we developed a calibration algorithm to improve accuracy, but further research should investigate the contribution of structural fires to other pollutants. The approach used here could also be extended, with assumptions regarding structure composition and combustion efficiency, to estimate the total mass of structure burned. Second, our results refer to average effects, but we observe considerable variation across fires. We rely on the complete population of fires both to account for confounding factors that may affect any one fire and because there were relatively few sensors downwind of fires: although we examine

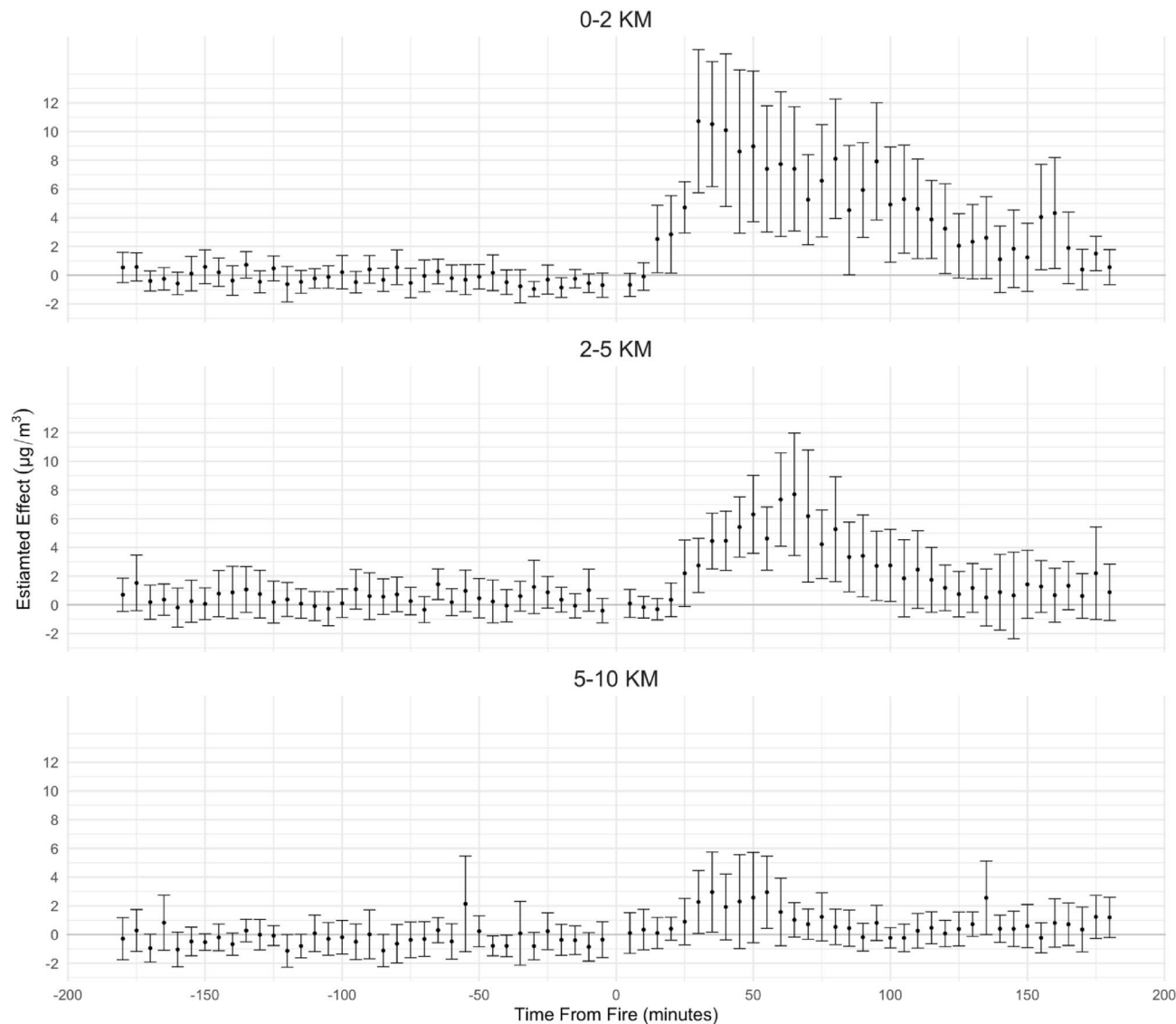


Figure 5. Model-estimated effect of structural fires on PM_{2.5} by distance from fire. Estimates are from models including time and sensor-specific fixed effects and meteorological parameters, with standard errors clustered by sensor. Number of Fires = 21. Number of downwind sensors = 16 (0–2 km), 13 (2–5 km), 11 (5–10 km).

	Downwind Band CBGs		Non-Downwind Band CBGs		T-statistic	P-value
	Mean	SE	Mean	SE		
Median income	64,066	1724	70,745	979	-3.50	< 0.001
Percent White	27.1	1.2	36.6	0.8	-6.31	< 0.001
Percent Black	38.7	1.7	28.2	1.0	5.59	< 0.001
Percent Hispanic	24.8	1.1	27.5	0.8	-1.85	0.06
Percent over 65	13.2	0.4	13.5	0.2	-0.81	0.42
Percent under 6	7.4	0.2	6.5	0.1	3.62	< 0.001
	n = 586		n = 1525			

Table 1. Socioeconomic and demographic characteristics of census block groups (CBGs). Results of two-tailed t-test comparing CBGs that fall into at least one of the downwind bands versus those that do not. (df = 2109).

21 fires in our study, only 14 had downwind sensors within 5 km, and the distance of those sensors from the fires varied considerably. Nevertheless, the network used in our study is among the largest and most spatially dense low-cost sensor networks deployed in any major city³⁶, and offers an important example of how these increasingly common networks can capture changes in PM_{2.5} concentrations associated with local events such as fires. Finally, we also make several simplifying assumptions in our methodology. In particular, the rectangular downwind band is a relatively simple representation of a fire plume and does not consider neighborhood-level wind speed or the urban form of the area impacted by the fire; however, our results are robust to sensitivity analyses using bands representing the fire's emissions paths of various widths (600 m, 1400 m, 2000 m). Similarly, our meteorological information is limited to that of the two national weather stations in the city and we assume that wind direction is consistent across the metropolitan area and persistent over the 3 hours before and after each fire's start. Future work should examine how street canyons and other elements of urban form complicate these assumptions.

Nevertheless, our study demonstrates the value of large-scale, low-cost sensor networks in characterizing previously under-monitored urban phenomena. Although an extensive literature documents the disproportionate long-term pollution burdens borne by low-income people and people of color^{58–61}, our research offers novel evidence that short-term events follow similarly inequitable patterns. We also highlight the impact of localized events on vulnerable populations such as schoolchildren; future work could build upon these insights to develop real-time and geolocated warning systems that support targeted public health warning systems.

Data availability

All data for this study are collected from publicly available sources including Microsoft Project Eclipse⁶², the Chicago Fire Department's public twitter account³⁸, NOAA⁴⁰, the U.S. Census Bureau⁵⁰, and the Chicago Open Data Portal^{51,52}. The cleaned analytic data are available from the corresponding author upon request.

Received: 17 February 2023; Accepted: 7 July 2023

Published online: 08 August 2023

References

- Vos, T. *et al.* Global burden of 369 diseases and injuries in 204 countries and territories, 1990–2019: A systematic analysis for the global burden of disease study 2019. *The Lancet* **396**, 1204–1222 (2020).
- World Health Organization. Billions of people still breathe unhealthy air: New who data. <https://www.who.int/news/item/04-04-2022-billions-of-people-still-breathe-unhealthy-air-new-who-data> (2022).
- Al-Kindi, S. G., Brook, R. D., Biswal, S. & Rajagopalan, S. Environmental determinants of cardiovascular disease: Lessons learned from air pollution. *Nat. Rev. Cardiol.* **17**, 656–672 (2020).
- Pozzer, A. *et al.* Regional and global contributions of air pollution to risk of death from covid-19. *Cardiovasc. Res.* **116**, 2247–2253 (2020).
- Klepac, P., Locatelli, I., Korošec, S., Künzli, N. & Kukec, A. Ambient air pollution and pregnancy outcomes: A comprehensive review and identification of environmental public health challenges. *Environ. Res.* **167**, 144–159 (2018).
- Bekkar, B., Pacheco, S., Basu, R. & DeNicola, N. Association of air pollution and heat exposure with preterm birth, low birth weight, and stillbirth in the US: A systematic review. *JAMA Netw. Open* **3**, e208243–e208243 (2020).
- Burnett, R. *et al.* Global estimates of mortality associated with long-term exposure to outdoor fine particulate matter. *Proc. Natl. Acad. Sci.* **115**, 9592–9597 (2018).
- Pope, C. A. III. & Dockery, D. W. Health effects of fine particulate air pollution: Lines that connect. *J. Air Waste Manag. Assoc.* **56**, 709–742 (2006).
- Deryugina, T., Heutel, G., Miller, N. H., Molitor, D. & Reif, J. The mortality and medical costs of air pollution: Evidence from changes in wind direction. *Am. Econ. Rev.* **109**, 4178–4219 (2019).
- Li, J. C. & Casher, D. The impact of an urban scrapyards fire on respiratory-related pediatric emergency department visits. *J. Occup. Environ. Med.* **62**, 764–770 (2020).
- Shah, A. S. *et al.* Short term exposure to air pollution and stroke: Systematic review and meta-analysis. *BMJ* **350**, 1 (2015).
- Borgschulte, M., Molitor, D. & Zou, E. *Air Pollution and the Labor Market: Evidence from Wildfire Smoke* (Tech. Rep., National Bureau of Economic Research, 2022).
- Link, M. S. *et al.* Acute exposure to air pollution triggers atrial fibrillation. *J. Am. Coll. Cardiol.* **62**, 816–825. <https://doi.org/10.1016/j.jacc.2013.05.043> (2013).
- Liang, Y. *et al.* Wildfire smoke impacts on indoor air quality assessed using crowdsourced data in California. *Proc. Natl. Acad. Sci.* **118**, e2106478118 (2021).
- Barwick, P. J., Li, S., Lin, L. & Zou, E. *From Fog to Smog: The Value of Pollution Information* (Tech. Rep., National Bureau of Economic Research, 2019).
- McLaughlin, T., Kearney, L. & Sanicola, L. Special report: U.S. air monitors routinely miss pollution—Even refinery explosions. Tech. Rep., Reuters (2020).
- Zou, E. Y. Unwatched pollution: The effect of intermittent monitoring on air quality. *Am. Econ. Rev.* **111**, 2101–26 (2021).
- Hsu, Y.-C. *et al.* Community-empowered air quality monitoring system. In *Proceedings of the 2017 CHI Conference on Human Factors in Computing Systems*, 1607–1619 (2017).
- Chen, Y. *et al.* A new mobile monitoring approach to characterize community-scale air pollution patterns and identify local high pollution zones. *Atmos. Environ.* **272**, 118936. <https://doi.org/10.1016/j.atmosenv.2022.118936> (2022).
- Chen, L.-J. *et al.* Adf: An anomaly detection framework for large-scale pm2.5 sensing systems. *IEEE Internet Things J.* **5**, 559–570. <https://doi.org/10.1109/JIOT.2017.2766085> (2018).
- Rassam, M. A., Zainal, A. & Maarof, M. A. Advancements of data anomaly detection research in wireless sensor networks: A survey and open issues. *Sensors* **13**, 10087–10122. <https://doi.org/10.3390/s130810087> (2013).
- Bosman, H. H., Iacca, G., Tejada, A., Wörtche, H. J. & Liotta, A. Spatial anomaly detection in sensor networks using neighborhood information. *Inf. Fus.* **33**, 41–56. <https://doi.org/10.1016/j.inffus.2016.04.007> (2017).
- Ahrens, M. & Everts, B. *Fire Loss in The United States During 2020* (Tech. Rep., National Fire Protection Association, 2021).
- Shie, R.-H. & Chan, C.-C. Tracking hazardous air pollutants from a refinery fire by applying on-line and off-line air monitoring and back trajectory modeling. *J. Hazard. Mater.* **261**, 72–82. <https://doi.org/10.1016/j.jhazmat.2013.07.017> (2013).
- Liu, G. *et al.* Chemical explosion, Covid-19, and environmental justice: Insights from low-cost air quality sensors. *Sci. Total Environ.* **849**, 157881 (2022).
- Griffiths, S. D., Chappell, P., Entwistle, J. A., Kelly, F. J. & Deary, M. E. A study of particulate emissions during 23 major industrial fires: Implications for human health. *Environ. Int.* **112**, 310–323. <https://doi.org/10.1016/j.envint.2017.12.018> (2018).

27. Jennings, C. R. Social and economic characteristics as determinants of residential fire risk in urban neighborhoods: A review of the literature. *Fire Saf. J.* **62**, 13–19 (2013).
28. Turner, S. L. *et al.* Risk factors associated with unintentional house fire incidents, injuries and deaths in high-income countries: A systematic review. *Inj. Prev.* **23**, 131–137 (2017).
29. Samet, J. M., Dominici, F., Currier, I., Coursac, I. & Zeger, S. L. Fine particulate air pollution and mortality in 20 US cities, 1987–1994. *N. Engl. J. Med.* **343**, 1742–1749 (2000).
30. Jaffe, D. A. *et al.* Wildfire and prescribed burning impacts on air quality in the United States. *J. Air Waste Manag. Assoc.* **70**, 583–615 (2020).
31. Fent, K. W. *et al.* Airborne contaminants during controlled residential fires. *J. Occup. Environ. Hyg.* **15**, 399–412 (2018).
32. Barkjohn, K. K., Gantt, B. & Clements, A. L. Development and application of a united states-wide correction for pm 2.5 data collected with the purpleair sensor. *Atmos. Measur. Tech.* **14**, 4617–4637 (2021).
33. Daepf, M. I. *et al.* The “three-legged stool”: Designing for equitable city, community, and research partnerships in urban environmental sensing. In *Proceedings of the 2023 CHI Conference on Human Factors in Computing Systems*, 1–19 (2023).
34. Matte, T. D. *et al.* Monitoring intraurban spatial patterns of multiple combustion air pollutants in New York city: design and implementation. *J. Expo. Sci. Environ. Epidemiol.* **23**, 223–231 (2013).
35. Duvall, R. *et al.* Performance testing protocols, metrics, and target values for fine particulate matter air sensors: Use in ambient, outdoor, fixed sites, non-regulatory supplemental and informational monitoring applications. US EPA Office of Research and Development (2021).
36. Daepf, M. I. *et al.* Eclipse: An end-to-end platform for low-cost, hyperlocal environmental sensing in cities. In *2022 21st ACM/IEEE International Conference on Information Processing in Sensor Networks (IPSN)*, 28–40 (IEEE, 2022).
37. Microsoft Research. Project eclipse data on the planetary computer. <https://planetarycomputer.microsoft.com/dataset/eclipse> (2022).
38. Chicago Fire Media. <https://twitter.com/CFDMedia>. Accessed 2022 July 2004.
39. Nominatim. Open-source geocoding with openstreetmap data. <https://nominatim.org>. Accessed 2022 June 25.
40. Meteostat. Data sources. <https://dev.meteostat.net/sources.html> (2021). Accessed 2022 July 2004.
41. Lu, Y., Giuliano, G. & Habre, R. Estimating hourly pm2.5 concentrations at the neighborhood scale using a low-cost air sensor network: A los angeles case study. *Environ. Res.* **195**, 110653. <https://doi.org/10.1016/j.envres.2020.110653> (2021).
42. Aldrin, M. & Haff, I. H. Generalised additive modelling of air pollution, traffic volume and meteorology. *Atmos. Environ.* **39**, 2145–2155. <https://doi.org/10.1016/j.atmosenv.2004.12.020> (2005).
43. Cichowicz, R., Wielgosiński, G. & Fetter, W. Effect of wind speed on the level of particulate matter pm10 concentration in atmospheric air during winter season in vicinity of large combustion plant. *Atmos. Chem.* **77**, 35–48. <https://doi.org/10.1007/s10874-020-09401-w> (2020).
44. Florida, R. *Skyscrapers, the pros and cons*. <https://www.bloomberg.com/news/articles/2016-01-28/skyscrapers-the-pros-and-cons> (2016).
45. Herman, C. *Street and site plan design standards—City of Chicago*. <https://www.chicago.gov/dam/city/depts/cdot/StreetandSitePlanDesignStandards407.pdf> (2021).
46. O'Brien, D. T. & Mueller, A. V. In pursuit of local solutions for climate resilience: Sensing microspatial inequities in heat and air pollution within urban neighborhoods in boston, ma. *Sustainability* **15**, 2984 (2023).
47. Wang, J. & Ogawa, S. Effects of meteorological conditions on PM2.5 concentrations in Nagasaki, Japan. *Int. J. Environ. Res. Public Health* **12**, 9089–9101. <https://doi.org/10.3390/ijerph120809089> (2015).
48. Sun, R., Zhou, Y., Wu, J. & Gong, Z. Influencing factors of PM2.5 pollution: Disaster points of meteorological factors. *Int. J. Environ. Res. Public Health* **16**, 3891. <https://doi.org/10.3390/ijerph16203891> (2019).
49. Baldi, M. *et al.* Analysis of the influence of precipitation and wind on pm2.5 and pm10 in the atmosphere. *Adv. Meteorol.* <https://doi.org/10.1155/2020/5039613> (2020).
50. U. S. Census Bureau. 2016–2020 American Community Survey 5-year estimates detailed tables. <https://www.census.gov/data/developers/data-sets/acs-5year.html>. Accessed 2022 August 2010.
51. City of Chicago. Chicago Public Schools—School locations SY2021. <https://data.cityofchicago.org/Education/Chicago-Public-Schools-School-Locations-SY2021/p83k-txqt/data>. Accessed 2022 August 2010.
52. City of Chicago. Senior centers. <https://data.cityofchicago.org/Health-Human-Services/Senior-Centers/qhfc-4cw2>. Accessed 2022 August 10.
53. Pope, C. A. *et al.* Short-term exposure to fine particulate matter air pollution is preferentially associated with the risk of ST-segment elevation acute coronary events. *J. Am. Heart Assoc.* **4**, 1 (2015).
54. Do, K. *et al.* A data-driven approach for characterizing community scale air pollution exposure disparities in inland southern california. *J. Aerosol. Sci.* **152**, 105704 (2021).
55. Wang, Q., Phillips, N. E., Small, M. L. & Sampson, R. J. Urban mobility and neighborhood isolation in America's 50 largest cities. *Proc. Natl. Acad. Sci.* **115**, 7735–7740 (2018).
56. Adamkiewicz, G. *et al.* Moving environmental justice indoors: Understanding structural influences on residential exposure patterns in low-income communities. *Am. J. Public Health* **101**, S238–S245 (2011).
57. Morawska, L. *et al.* Applications of low-cost sensing technologies for air quality monitoring and exposure assessment: How far have they gone?. *Environ. Int.* **116**, 286–299. <https://doi.org/10.1016/j.envint.2018.04.018> (2018).
58. Goldizen, F. C., Sly, P. D. & Knibbs, L. D. Respiratory effects of air pollution on children. *Pediatr. Pulmonol.* **51**, 94–108. <https://doi.org/10.1002/ppul.23262> (2015).
59. Tessum, C. W. *et al.* PM 2.5 pollutants disproportionately and systemically affect people of color in the united states. *Sci. Adv.* **7**, <https://doi.org/10.1126/sciadv.abf4491> (2021).
60. Di, Q. *et al.* Air pollution and mortality in the medicare population. *N. Engl. J. Med.* **376**, 2513–2522. <https://doi.org/10.1056/nejmoa1702747> (2017).
61. Jbaily, A. *et al.* Air pollution exposure disparities across US population and income groups. *Nature* **601**, 228–233. <https://doi.org/10.1038/s41586-021-04190-y> (2022).
62. Microsoft Research Urban Innovation Eclipse Sensor Data. <https://planetarycomputer.microsoft.com/dataset/eclipse>. Accessed July 2022.

Acknowledgements

The authors thank Scott Filion and Anastasia Montgomery for their feedback. We are also grateful to Charles Needham, Jr, Lex Story, Darren Gehring, Gavin Jancke, Asta Roseway, and Scott Counts for their critical support and to Tiffany Werner, Raed Mansour, and Susan Mudd for key feedback. This work was funded internally by Microsoft.

Author contributions

A.A.: Conceptualization, Methodology, Writing—Original Draft Preparation. A.C.: Methodology, Data Curation, Writing- Reviewing and Editing. M.I.A.: Methodology, Writing—Review and Editing. P.C.: Data Curation,

Writing—Reviewing and Editing. M.I.G. Daep: Supervision, Methodology, Writing—Original Draft Preparation, Review, and Editing.

Competing interests

The authors declare no competing interests.

Additional information

Supplementary Information The online version contains supplementary material available at <https://doi.org/10.1038/s41598-023-38392-3>.

Correspondence and requests for materials should be addressed to A.A.

Reprints and permissions information is available at www.nature.com/reprints.

Publisher's note Springer Nature remains neutral with regard to jurisdictional claims in published maps and institutional affiliations.



Open Access This article is licensed under a Creative Commons Attribution 4.0 International License, which permits use, sharing, adaptation, distribution and reproduction in any medium or format, as long as you give appropriate credit to the original author(s) and the source, provide a link to the Creative Commons licence, and indicate if changes were made. The images or other third party material in this article are included in the article's Creative Commons licence, unless indicated otherwise in a credit line to the material. If material is not included in the article's Creative Commons licence and your intended use is not permitted by statutory regulation or exceeds the permitted use, you will need to obtain permission directly from the copyright holder. To view a copy of this licence, visit <http://creativecommons.org/licenses/by/4.0/>.

© The Author(s) 2023